

Inkjet-Printed Graphene-Based Wireless Gas Sensor Modules

Taoran Le¹, Vasileios Lakafosis¹, Ziyin Lin², C. P. Wong², and M. M. Tentzeris¹

¹School of ECE, ²School of Materials Science and Engineering,

Georgia Institute of Technology

Atlanta, GA 30332

taoran.le@ece.gatech.edu

Abstract

In this paper we demonstrate the use of graphene as the basis for design and development of low-cost, self-powered, battery-less, wireless sensor solutions utilizing thin films produced from environmentally friendly, water-based, inkjet printed graphene oxide (GO) ink. The in-house developed novel sensor material demonstrates good response to ammonia gas (NH₃), yielding a 6% normalized resistance change within 15 minutes of exposure to a concentration of 500 ppm. In addition, excellent recovery time is achieved using the RGO thin films, with over 30% of material recovery observed within 5 minutes without exposure to high temperature or any UV treatments. Finally, we present in this work important distinctive characteristics in the behavior of the RGO sensor when exposed to different types of gases, including the hard-to-detect CO gas, that can be exploited in order to further enhance the applicability of the material. The introduction of mass producible, stable, environmentally friendly, inkjet-printable GO on organic paper / kapton substrates lays the foundation for the development of a wide range of new low-cost, high performance graphene-based devices, such as inkjet-printed diodes, capacitors and transistors.

Index Terms — Gas sensor, graphene, inkjet printing, RGO, thin films, RFID.

Introduction

The early and accurate detection of hazardous chemicals is advantageous for both industrial use and for environmental cognition, and is of benefit to both the public and private sectors. Recent advances in materials science have led to the employment of novel nano-materials, such as carbon nanotube (CNT) and graphene, for chemical sensing applications. These materials alter their properties in the presence of a given substance due to their ability to absorb the chemicals on their surface.

Chemical absorption produces changes in material properties such as real and imaginary impedance, DC resistance, and effective dielectric constant [1]. These changes can be exploited to determine the presence of various chemical compounds by translating the material effects into measurable electrical quantities, such as changes in voltage, current, resonant frequency, and backscattered power amplitude. Excellent electrical conductivity and the ability to be functionalized for a wide range of chemicals make these novel materials ideal candidates for the development of a broad spectrum of portable and wearable sensors. Moreover, the ability to deposit these materials via inkjet printing of aqueous solutions on low cost, flexible, environmentally friendly substrates opens the possibility of mass producing such devices and taking advantage of economies of scale.

In our previous research efforts, we have demonstrated excellent gas detection sensitivity results for nitrogen-based gases [1]. At 10ppm NO₂ we achieved 21% sensitivity, and at 4ppm NH₃, 9% sensitivity was obtained at 864 MHz using functionalized multi walled CNT (MWCNT) dissolved in water and inkjet printed on paper substrate.

This study will consider the use of graphene as a means to enhance the performance of the devices, and as a means to introduce selectivity into the functionality of our previous gas sensor efforts. Graphene is a single planar layer of carbon atoms with exotic physical properties including high mobility of charge carriers (200,000 cm²V⁻¹s⁻¹), and high thermal conductivity (~5,000 Wm⁻¹K⁻¹). Most importantly, as a zero bandgap semiconductor, graphene's high metallic conductivity and low charge carrier density enable extreme sensitivity because small variations in charge carrier density yield notable changes in conductivity (single gas molecule detection has been demonstrated in a prototype device).

The paper will establish for the first time the principles of wireless gas sensor design utilizing graphene thin films and combining both analog (passive) and digital (battery-less semi-active) wireless remote transmission principles with graphene-based enhanced selectivity, featuring the first ever inkjet-printing of aqueous graphene solution on environmentally friendly paper and kapton substrates. Regarding in particular the digital transmission scenario, the coupling of gas sensing with power-efficient wireless data transmission is achieved by deploying Intel's Wireless Integrated Sensing Platform (WISP). The platform adds microcontroller functionality to traditional RFID tags, which operate as the sensor's integration platform. The WISP can be programmed to sample a variety of different responses and produce gas detection results taking advantage of additional processing, such as time-averaged stabilized or normalized difference gas-induced material changes.

Inkjet Printing of Graphene Sensor Prototype

The core of the wireless gas sensor is a prototype board made from graphene deposited onto a flexible substrate, in this case paper and kapton. Graphene was chosen for several reasons. First, it exhibits remarkable electronic and mechanical properties [2-4], and graphene oxide materials can be easily dispersed in water. In our previous work on CNT based wireless gas sensors, the short lifetime and poor dispersion of the CNT ink limited the obtainable material performance [1,5]. Additionally, due to the fact that graphene is an extremely low-noise material electronically, graphene offers clear advantages in terms of minimum detection levels to other solid-state gas sensors, such as those created from CNT [6].

Cabot conductive nanoparticle silver ink was used to create the traces connecting the graphene pad to the external

circuitry. We used Cabot's CCI-300 ink here, which contains surface modified ultra-fine silver nanoparticles, providing reliable inkjet printing of high-resolution and low resistivity conductive features on a variety of substrates [7]. Microstrip topology was used since the silver microstrip trace can be easily integrated with large range of inkjet printed antennas as noted in [5].

A. Creation of Graphene Oxide

The first step in the sensor development process was the creation of stable, long-life, inkjet-printable graphene-based inks. This was accomplished by first converting the graphene into graphene oxide powder. Unlike pristine graphene, which has very poor dispersion in common solvents, GO exhibits excellent solubility in water due to the existence of hydrophilic functional groups on the surface [8], rendering it an excellent candidate for development of environmental friendly water-based inks. After deposition, pure graphene was obtained by the reduction of GO, which reverts the conjugated basal plane and restores the electrical properties of the material. The reduction of GO is considered as one of most promising methods for low-cost, high-yield and scalable preparation of graphene materials [9].

The GO was produced by chemical oxidation of graphite, which introduces oxygen-containing functional groups to exfoliate pristine graphite into individual GO sheets. GO was prepared with Hummers' method [10]. Typically, graphite flake was placed into a NaNO_3 /concentrated H_2SO_4 solution in an ice bath. Subsequently, KMnO_4 was slowly added to the solution while maintaining the temperature $< 20^\circ\text{C}$. The mixture was stirred in the ice bath for 2 hours and for an additional 30 minutes in a 35°C water bath. After that, 70mL 70°C water was added slowly into the flask. The heat generated via exothermic reaction raised the solution temperature up to 98°C . Then additional 140mL 70°C water was added, followed by hydrogen peroxide solution to terminate the reaction. The mixture was filtrated and washed with water to remove excess acid and inorganic salts. The resulting GO was dried overnight at 55°C to produce the GO powder. To prepare the GO ink, dry GO powder was dispersed in a water/glycerol solution and sonicated to form a homogenous dispersion.

B. Fabrication via Inkjet Printing

A Dimatix Materials Printer (DMP-2800) Series material deposition system was used to print both the silver and GO inks. Before printing, the kapton substrate was treated by UV-Ozone to improve its hydrophilicity. The treated kapton demonstrated improved performance during printing compared to the native kapton substrate, enabling higher resolution prints and more layers to be printed during a given cycle.

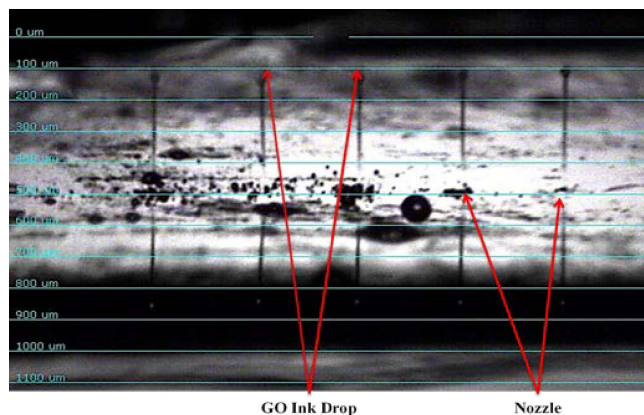


Figure 1. Graphene drop ejected from inkjet printer onto kapton substrate.

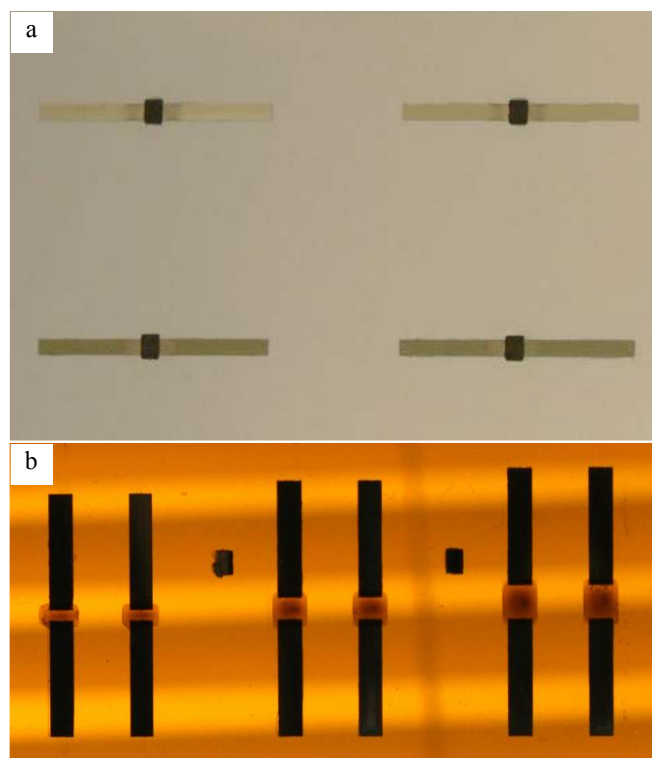


Figure 2. (a) Graphene-based thin films inkjet-printed in-between and overlapping silver conductive inkjet-printed trace on paper substrate. (b) Graphene oxide thin films inkjet-printed in-between and overlapping silver conductive inkjet-printed trace on kapton substrate.

The fabrication process involved deposition of 10 layers of conductive silver onto the kapton substrate, followed by 12 to 42 layers of graphene oxide. First, the 10 layers of silver ink were deposited and cured at 120°C for 8 hours. Next, 2 layers of GO were deposited and cured at 80°C for 4 hours to serve as a foundation for further prints. These 2 foundational layers overlapped the silver pads by 0.5mm to ensure optimum connectivity. Next, the GO was deposited in 5 layer increments with curing in between to ensure the highest consistency between samples. Fig. 1 above illustrates the printing of GO ink. Fig. 2 shows the completed sensor elements prior to reduction of the GO thin films.

C. Reduction of Graphene Oxide

After printing and curing, each sample was reduced to obtain the desired graphene from the GO. Due to the reduction process of graphene oxide, we fabricated the samples on kapton substrate. After thermal reduction, the resistance became as low as 150Ω , approximately 1000 times better than the performance mentioned in the current literature [11]. Reduction was achieved by placing the printed GO thin films in elevated temperature in a hydrogen and argon atmosphere. The samples were reduced at 200°C for 30 min and 300°C for another 30 min. The heating rate was $5^\circ\text{C}/\text{min}$. After reduction, the samples were left to cool down to room temperature naturally. Scanning electron microscopy (SEM) was used to determine the overall quality of the graphene thin films (i.e. presence of defects in the print, etc.), and to make adjustments in processing to further prints. Fig. 3 below provides SEM images of both the initial GO and (reduced) RGO thin films. The wrinkles on the surface of the samples in Fig. 3 are typical characteristics of GO and RGO thin films, which are likely indicative of minor defects in the structure.

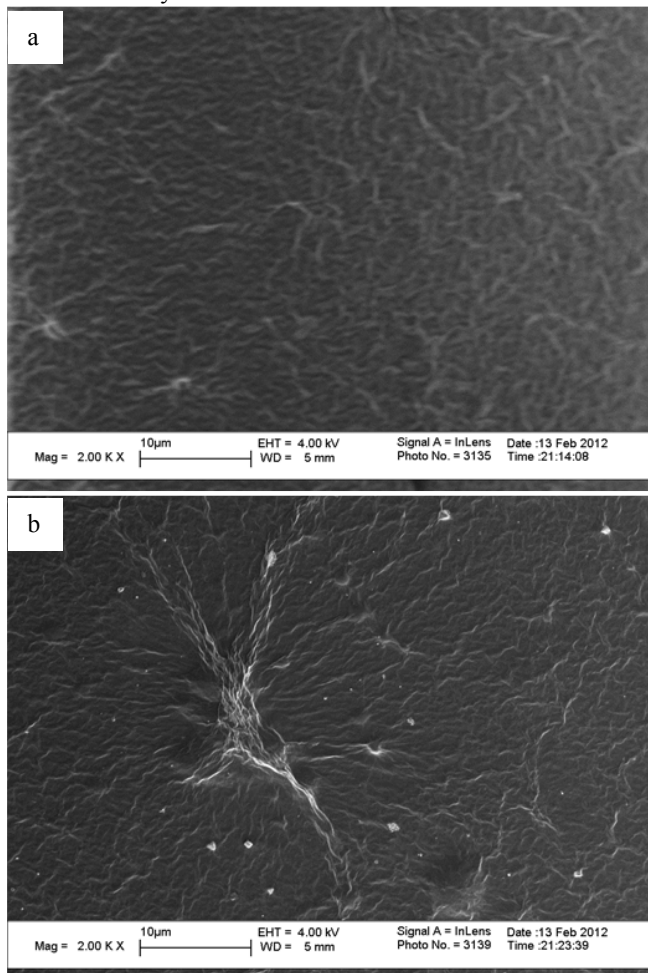


Figure 3. (a) SEM image of the inkjet printed GO thin film.(b) SEM image of the inkjet printed RGO thin film.

The examination on the whole patterned area revealed a uniform RGO layer with nearly 100% coverage, indicating the high quality of the GO layer obtained from the inkjet printing process and the fact that the reduction process doesn't bring significant change in the morphology of printed graphene.

D. Final Packaging Steps

One important fabrication factor, which was explored in the framework of this work, was the impact of the contact between silver and graphene on the system performance. Based on experimentation, we determined that the application of additional 10 layers of silver applied on top of the graphene guarantees better connectivity between the graphene and silver traces and helps to de-embed any additional impedance which would offset the measured change of impedance unevenly among different samples of the similar dimensions. We perform this important step as a means to reduce the variability between samples.

Optimization of the Reduced Graphene Oxide Thin Film

Optimization of the RGO thin films was done in order to obtain the proper sensor area to ensure maximum sensitivity while obtaining the requisite intrinsic impedance to ensure proper operation of the sensor board of the wireless platforms presented in Section "Wireless Transmission of Sensed Information".

To determine the optimum sensor area, three patterns of differing lengths of RGO material were produced, as shown in Fig. 2(b). It was expected that the larger surface area of the last pattern would yield the highest sensitivity. Based on previous efforts on thin film design, it was estimated that between 15-25 layers of the material would be necessary to achieve the desired resistance for the given dimensions of the RGO pads. To validate this assertion, samples of both 15 and 25 layer versions of the patterns were printed and reduced. The measured results can be found in Table 1 below. These values represent the average resistance values for a given combination of RGO pad dimension and thickness (# layers).

TABLE 1: AVERAGE INTRINSIC RESISTANCE VALUES OF RGO THIN FILMS.

# LAYERS	PATTERN 1	PATTERN 2	PATTERN 3
15	501.9 Ω	1123.8 Ω	2014.8 Ω
25	248.2 Ω	488.0 Ω	881.8 Ω

Gas Sensor Experimentation

A. Experiment Setup

The gas test setup is shown in Fig. 4 below. The sensors were tested using an Environics® S4000 gas mixing system. The setup was capable of producing reliable mixtures up to 500 ppm of ammonia gas diluted in air and delivered at a rate of 50 ccm. To calibrate the sensor, the graphene samples were placed into a semi-closed glass chamber to direct the flow of gas across the sensor. The custom designed gas flowing chamber, shown in Fig. 5, has internal dimensions of 4cm x 1.5cm x 1.5cm.

Air was flowed through the system for 15 minutes to establish a system baseline. Next, the gas mixture (500 ppm of ammonia/air or 0.1% CO/air) was introduced into the system and measurements of the resistance were taken at one-minute intervals for 15 minutes until near steady state

condition in the material was achieved. Finally, the gas source was removed from the device while measurements continued to be taken for another 15-minute interval in order to measure the recovery time.

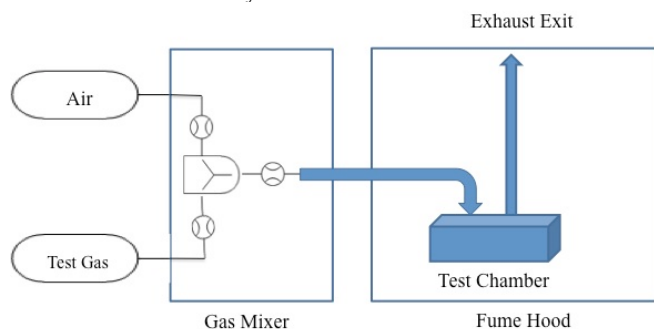


Figure 4. Measurement setup to test the RGO thin films.

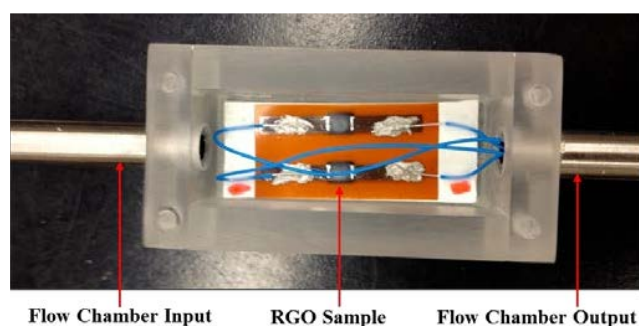


Figure 5. Test chamber with 2 samples inside.

B. Experimental Results

The results of 500ppm NH_3 gas testing are shown in Fig.6. The inkjet-printed RGO thin films of different dimensions show similar responses to 500 ppm NH_3 . The electrical resistance rapidly increases in the first few minutes after the introduction of NH_3 , indicating a fast detection rate. With the continued supply of NH_3 , the resistance change begins to diminish after 10 minutes, which occurs as the material enters the saturation region.

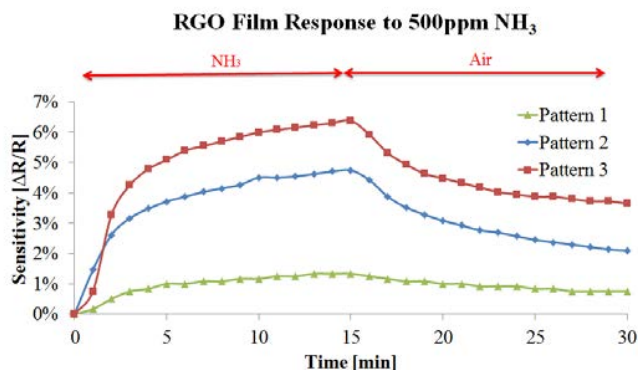


Figure 6. Measured response of RGO thin films in presence of NH_3 .

The maximum sensitivity is observed in the case of pattern 3, which shows greater than 6 % increase in normalized resistance. The effect of the RGO pattern dimension on the sensor performance is still under investigation. Here, it was observed that the pattern with largest area provided the best

result. After the introduction of NH_3 , pure air was introduced into the system and it was found that the resistance quickly recovered a large portion of its original value (~30%) within 5 minutes.

The increase in resistance upon exposure to NH_3 is due to the electron donation of NH_3 to the p-type RGO film, and is consistent with the literature. Compared to other works on graphene-based gas sensors, our inkjet printed RGO demonstrates superior performance, including a high sensitivity, fast response and quick recovery. Particularly, the short recovery time in natural environmental conditions is hugely advantageous over other reports which used UV and heat treatment to assist the recovery, and is of great importance for practical applications [6]. The sensor exhibits an observable (~10 Ω) change in resistance within one minute after introducing NH_3 , a measure which is certainly in the detectable range of the backend circuitry of the WISP platform.

The measured response of the material to CO gas is shown in Fig. 7 below. Here, the RGO thin film was exposed to 0.1% CO. This concentration was necessary to invoke response of the material. For the comparison between CO and NH_3 testing results, we plot the results of the pattern 3 samples together. The sensitivity for CO gas is substantially lower than that of NH_3 , which is similar as previous reports [6]. However, the important difference, which may potentially be used to differentiate between the two gases, is the unique response given by the CO gas. Note that the exposure to CO gas does not provide the same monotonic response as for NH_3 . Although the samples had some variance as noted above, each of the 8 samples tested under CO gas conditions contained the same rapid rise and fall while still under influence of the gas. As we have found only a few works in the literature concerning testing of inkjet printed RGO thin films with CO gas, we have little basis for comparison. However, the relevant sample size obtained during the experiments demonstrates that the effect is repeatable enough to be considered useful for the potential selectivity between different gases. Further experiments are ongoing to determine the significance of the observed phenomenon.

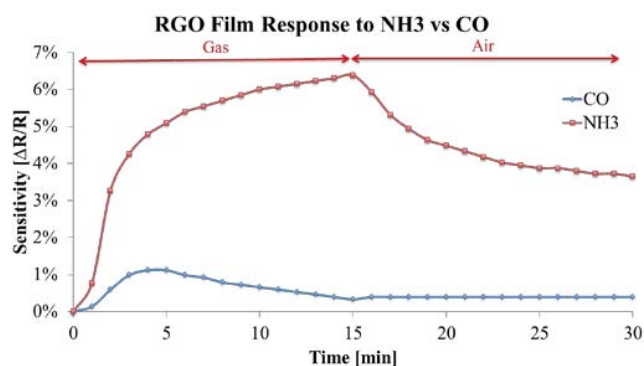


Figure 7. Measured response of RGO thin films to NH_3 and CO.

Wireless Transmission of Sensed Information

A. Analog Transmission

The incorporation of our novel graphene-based sensor thin films with micro-strip lines, as shown in Fig. 2, at this early

development stage only serve as a proof of concept. Of course these transmission lines can be thought of as parts of a wide range of antenna and microwave structures. For instance, the graphene micro-strip lines can be parts of the meander line of a bowtie antenna or even parts of short lines of micro-strip patch antennas [1], such as that shown in Fig. 8. Under this approach of analog transmission, the wireless remote sensing mechanism is actually the detection of the shift of the resonant frequency and / or the magnitude of the backscattered power as a direct result of the change of the impedance of the graphene stripes and, thus, also of the whole structure. Calibration may be needed in order to map particular amounts of shift in the resonant frequency or change in backscattered power to the concentration of toxic gases under test.

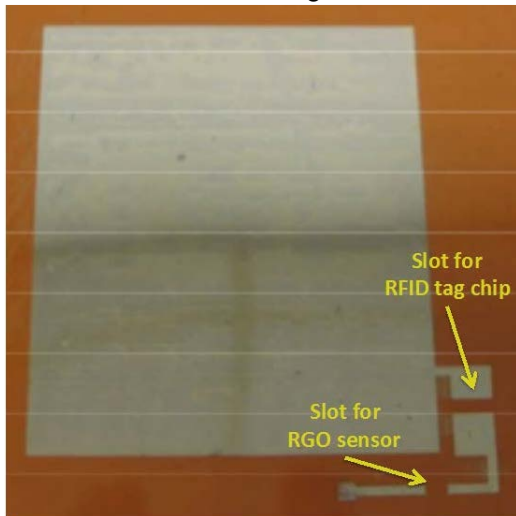


Figure 8. Inkjet Printed Antenna for development of analog gas sensor.

Regarding the range of frequencies that can be supported through these types of antenna structures, this ultimately depends on both the manufacturing accuracy of these transmission lines and, on the other hand, on how thin the graphene lines can be fabricated while still maintaining high levels of sensitivity. Preliminary results toward that direction demonstrate that it is the surface area of the inkjet-printed graphene and not the number of its inkjet-printed layers that determine the sensitivity to the presence of small concentrations of poisonous gases. In other words, as long as the surface area of the RGO exposed to the air remains constant, regardless of the width of the lines that the RGO is part of, the gas sensitivity remains the same.

B. Digital Transmission

As opposed to the aforementioned analog-based transmission of the sensed information that might be subject to distortion due to the dynamic nature of the air medium, the WISP-GS (Gas Sensor) prototype that we have developed, shown in Fig. 9, offers the reliability of wireless digital transmission.

The WISP is a fully passive, battery-free and programmable RFID Tag [12], which can be powered and read by off-the-shelf EPC Gen2 UHF RFID Readers and has an on-board microcontroller for sensing and computing functions. In this work, we modify (hardware- and software-wise) the WISP to create a sensing and communication

platform which enables for the first time the introduction of gas sensing capabilities to RFID tags. The WISP-GS is solely powered by the RF energy illuminated by any commercial RFID Reader. This 915MHz RF energy is rectified with a charge pump topology of diodes and capacitors to charge the on-board capacitor. Whenever located within the interrogation zone of an RFID reader, the WISP-GS is automatically detected and begins transmission of the sensed information within the EPC message of the RFID communication.

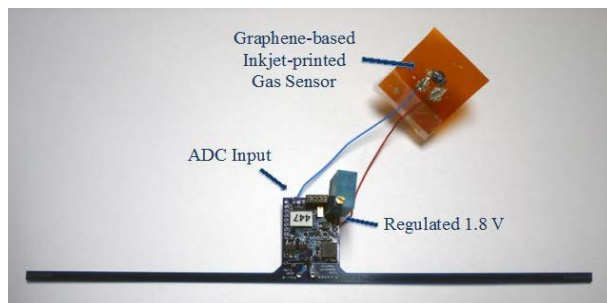


Figure 9. The WISP-GS (Gas Sensor) prototype platform

The external WISP-GS board consists, of course, of the graphene-based inkjet-printed RGO sensor, presented in the previous section, as well as the analog interface of this sensor. It is due to this analog interface, consisting essentially of a voltage divider, that the gas detection takes place locally at the end device level in terms of a simple impedance measurement and can be relayed digitally.

Future Work

During the gas flow periods, the inkjet printed RGO thin films reveal interesting responses. However, to enhance the usefulness of the material and to increase the accuracy of prediction, a larger sample size will be required to determine the exact “fingerprint” of the CO gas in comparison to other similar gases. In addition, more research is needed to explain the phenomena observed from a physical point of view. While it is well known that CO always acts as an electron donator to graphene, it is not understood how this mechanism can lead to the responses observed during this initial set of experiments [13].

Conclusion

We have demonstrated here the usefulness of graphene based thin films as a complement to wireless sensing technologies, highlighting their unique properties and ease of integration with existing wireless packaging technologies such as inkjet printing. We also provide detailed results of our efforts in the development of environmentally friendly, stable, low cost, inkjet-printable GO inks.

The prototype device exceeded our expectations for initial tests, producing a 6% change in resistance at 500 ppm concentration of ammonia gas. Moreover, the sensor demonstrated fast recovery time in comparison to the current state of technology without the use of heat or UV treatments to assist in the material recovery. These results can be improved upon by optimization of the deposition and curing

techniques, and with enhancements to the output circuitry of the final sensor design.

Our developed novel inks may soon provide the foundation for advancements in high-performance inkjet-printed electronics, such as inkjet-printed graphene based diodes, super capacitive devices, and transistors.

Acknowledgments

The authors would like to thank NSF-ECS and IFC-SRC for their support for the research.

References

1. V. Lakafosis et al., "Wireless Sensing with Smart Skins", IEEE Sensors 2011, pp. 623-626.
2. K.S. Novoselov et al., "The Rise of Graphene", Nat. Mater, 2007,6, pp.183-191.
3. D. Li et al., "Graphene-Based Materials", Science, 320, pp.1170-1171, 2008.
4. A. A. Balandin et al., "Superior Thermal Conductivity of Single-layer Graphene", Nano Letters, 2008, vol. 8 ISSU 3, pp. 902-907.
5. Y.Li et al., "A novel conformal RFID-enabled module utilizing inkjet-printed antennas and carbon nanotubes for gas-detection applications", IEEE Antennas and Wireless Propagation Letters [1536-1225],2009, vol.8.
6. F.Schedin et al., "Detection of individual gas molecules adsorbed on graphene" Nature Materials Vol.6, 2007.
7. <http://www.cabot-corp.com/CCI-300> Data Sheet.
8. Z. Lin et al., "Solvent-Assisted Thermal Reduction of Graphite Oxide," The Journal of Physical Chemistry C, pp. 14819-14825, 2010.
9. Z. Lin et al., "Ultrafast, dry microwave synthesis of graphene sheets," J. Mater. Chem., 2010, 20, pp. 4781-4783.
10. W. S. Hummers and R. E. Offeman, "Preparation of Graphitic Oxide," Journal of the American Chemical Society, vol. 80,(1958) pp. 1339-1339.
11. L. Le et al., "Graphene supercapacitor electrodes fabricated by inkjet printing and thermal reduction of graphene oxide," Electrochemistry Communication 13, pp. 355 -358, 2011.
12. A. Sample et al., "Design of an RFID-based battery-free programmable sensing platform," IEEE Transactions on Instrumentation and Measurement, pp. 2608 —2615, 2008.
13. O. Leenaets et al., "Adsorption of H₂O, NH₃, CO, NO₂, and NO on graphene: A first-principles study", Physical review. B, Condensed matter and materials physics [1098-0121],Vol.77, ISS.12,2008.